17th World Conference on Earthquake Engineering, 17WCEE
Sendai, Japan - September 13th to 18th 2020

CALCULATION METHOD OF INITIAL STIFFNESS FOR AN INNOVATIVE RESILIENT ROCKING COLUMN

Yang Liu[(1)], Rachel Chicchi[(2)], Zi-xiong Guo[(3)]

[(1)] *Professor, College of Civil Engineering, Huaqiao University, Xiamen, China, lyliuyang@hqu.edu.cn*
[(2)] *Assistant Professor, Department of Civil and Architectural Engineering and Construction Management, University of Cincinnati, Cincinnati, OH USA, rachel.chicchi@uc.edu*
[(3)] *Professor, College of Civil Engineering, Huaqiao University, Xiamen, China, gzxcy@hqu.edu.cn*

Abstract

Moment frame structures subjected to earthquakes are generally designed to dissipate energy through inelastic behavior at beam ends and column bases. In recent years, the structural engineering community has moved towards the design of resilient structures, which minimize this damage and allow for a return to building occupancy shortly after the seismic event. To address resilience, an innovative resilient rocking (IRR) column was designed. This IRR column consists of a column, which rocks about its base and steel slit dampers, which attach the rocking column to the foundation. Steel slit dampers are also used to dissipate energy and concentrate damage during a seismic event. This system has been experimentally and analytically studied in previous work. The IRR columns were found to display stable hysteretic behavior and inelastic behavior was concentrated to the dampers which can easily be removed and replaced. A simplified model using elastic beams and spring elements was established and the principle of energy conservation was employed in order to calculate the initial stiffness of the IRR column. The calculated initial stiffness of the IRR columns using the proposed method was verified with test and FE analysis results.

Keywords: Rocking columns, Replaceable steel slit dampers, Calculation method, Initial stiffness, Resilient structures

1. Introduction

Buildings today are typically designed to undergo inelastic (plastic) deformations in high seismic events in order to dissipate energy and prevent collapse. These plastic deformations, however, can cause unrecoverable damage and permanent residual drift in a structure, which may result in suspended building operations as the structure is repaired or demolished and rebuilt. Recognizing the desire for immediate occupancy and continued operability following a seismic event, the structural engineering community has begun to design and implement resilient structural systems and components capable of dissipating energy while strategically limiting structural damage.

Two strategies for structural resilience are implementation of rocking systems and use of replaceable fuses. Rocking systems permit displacement of the system through rigid body rocking action that minimizes structural damage. This concept has been employed in a variety of seismic force-resisting systems using post-tensioning in connections to achieve self-centering: precast concrete frames (El-Sheikh et al. (1999)[1], Priestley et al. (1999)[2]), steel moment resisting frames (Ricles et al. (2001, 2002)[3,4], Christopoulos et al. (2002)[5]), and steel plate shear walls (Dowden et al. (2016)[6]). The other strategy of replaceable fuses allows for concentrated damage and energy-dissipation to take place in components that can be relatively easily replaced after a seismic event. Studies related to replaceable fuses include: replaceable steel coupling beams (Fortney et al. 2007[7], Shahrooz et al. 2018[8], Farsi et al. 2016[9], Ji et al. 2017[10,11]), moment

resisting frames (Shen et al. (2011)[12], Oh et al. 2009[13], Köken et al. 2015[14]), and eccentrically braced frames (Mansour et al. 2011[15]).

A number of structural steel systems have also been investigated that combine rocking, self-centering, and replaceable energy-dissipative fuses. These include: rocking beams and yielding base plates (Azuhata et al. 2004[16]) and steel braced frames with replaceable steel fuse plates (Eatherton et al. (2014)[17]) The proposed innovative resilient rocking (IRR) column system provides a unique approach to seismic resilience through both rocking systems and replaceable fuses.

A moment-resisting frame (MRF) structure designed with the "strong-column/weak-beam" philosophy may experience a structural mechanism during an earthquake, which results in plastic deformation at the beam ends and column bases. If feasible, these damaged components may be replaced; however, replacement of column hinges is a difficult and costly process due to the gravity loads on the structure. The proposed IRR system employs a "strong-column/weak-damper" philosophy, which permits plastic behavior within replaceable fuses and ensures elastic behavior in the column, as shown in Fig. 1. The dampers connect the column to the foundation using a connecting place and high strength bolts at the column and a T-shaped steel plate with anchor bolts to attach to the foundation. The tube column is not directly attached to the foundation. When the column rocks, shear deformation in the dampers is initiated and the moment induced at the column base is resisted by the dampers. Experimental testing of the proposed IRR column demonstrated reparability and favorable seismic performance (Liu et al. (2019)[18]). The IRR columns exhibited stable hysteretic performance even under large displacements and the damaged components could be replaced without difficulty after cyclic loading.

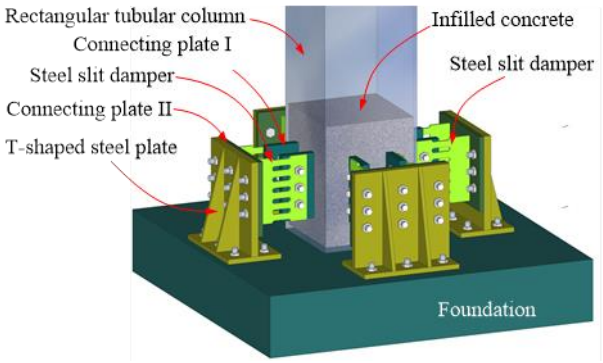

Fig. 1 – Schematic configuration of IRR column

2. Load transfer characteristics of IRR columns

The two steel slit dampers on each side of the column, which are oriented parallel to the horizontal loading direction, were considered, as shown in Fig. 2(a). The dampers that are oriented perpendicular to the loading direction were ignored and will be discussed in a future paper. As a horizontal load, P, is applied at the top of the column, the column rotates about the rotational point at the right bottom corner, which then causes an uplift of the steel slit dampers on the left side of the column, denoted as Damper L. There is also a small downward deflection of the right side connection plate, which is fastened with the right side steel slit damper, denoted as Damper R. This deflection is smaller than the left side due to the smaller distance from the rotational point to the edge of the damper compared with that of Damper L.

There are two kinds of simple deformation modes existing simultaneously in the steel slit dampers, which are shown in Fig. 2(b): the parallel shear deformation caused by only vertical displacement, δv (upward for Damper L and downward for Damper R); and rotation, α' (positive in clockwise direction), of the connection plate. Steel slit dampers under parallel shear deformation have been studied intensively (Climent et al. 1998[19], Chan et al. 2008[20], Lee et al. 2017[21]). These dampers behave similar to coupling beams in coupled wall structures with the inflection point at the middle and flexural hinges forming at the ends of the struts of the damper. However, it is the rotation of the connected plates that makes the calculation method more complex. Connection plate rotation is caused by the rotation of the rocking column.

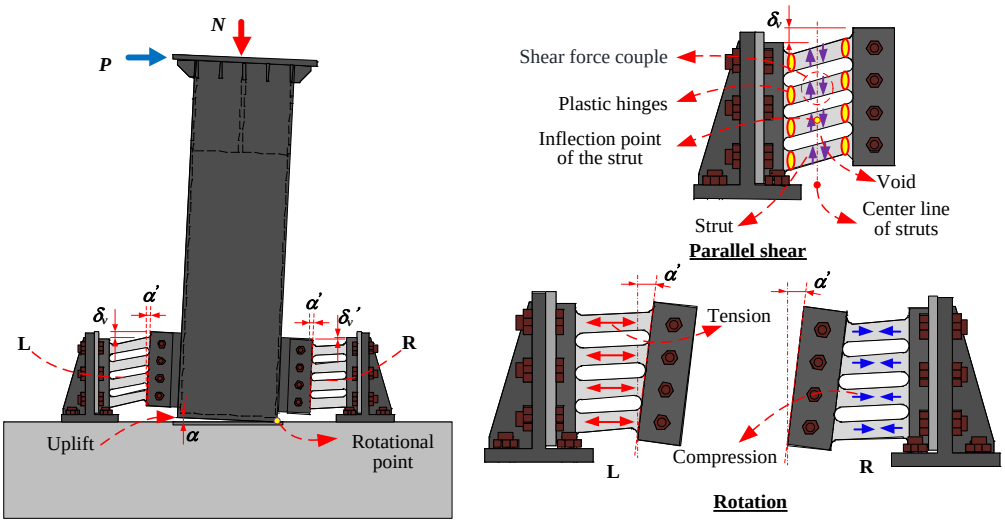

(a) Actual deformation (b) Two simple deformation modes

Fig. 2 – Deformation characteristics of IRR column and steel slit dampers

This rotation will result in tension and compression force in the struts, which will then contribute to the initial stiffness, as well as the moment resistance of the IRR column. It can be seen from Fig. 3 that the actual deformation mode of both steel slit dampers is the composition of these two deformation modes.

Some information and test results of one tested IRR column in previous study, S16-5.5-0.1, was shown in Fig. 3 to demonstrate the characteristics of the dampers and the overall seismic behavior of the IRR columns.

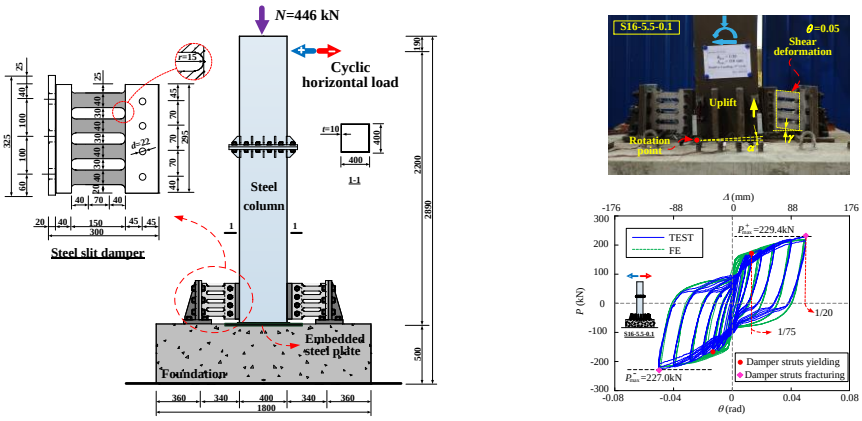

(a) Dimensions and details (b) Failure mode and hysteretic curve

Fig. 3 – Specimen information and test results of S16-5.5-0.1[18]

3. Calculation method of the initial stiffness of IRR columns

A simplified model was introduced based on the information of the tested IRR columns, as shown in Fig. 4, to derive the calculation equations of the initial stiffness of the specimens, where N and P are axial and horizontal load on the top of the column, respectively; H is the height from P to the top surface of the foundation; Δ is the horizontal displacement at the height P applied; a and b are width of the column and connection plates, respectively; L is the clear length of the struts; α is angle between the bottom face of the column and the top surface of the foundation. The following assumptions are adopted:

(1) No relative slippage is considered.

(2) Damper struts were simplified as a combination of an elastic beam element that does not transfer axial load and a spring element, as shown in the insert of Fig. 4.

(3) Steel column was simplified as an elastic cantilever beam with the fixed end at the height of the centroid of the dampers.

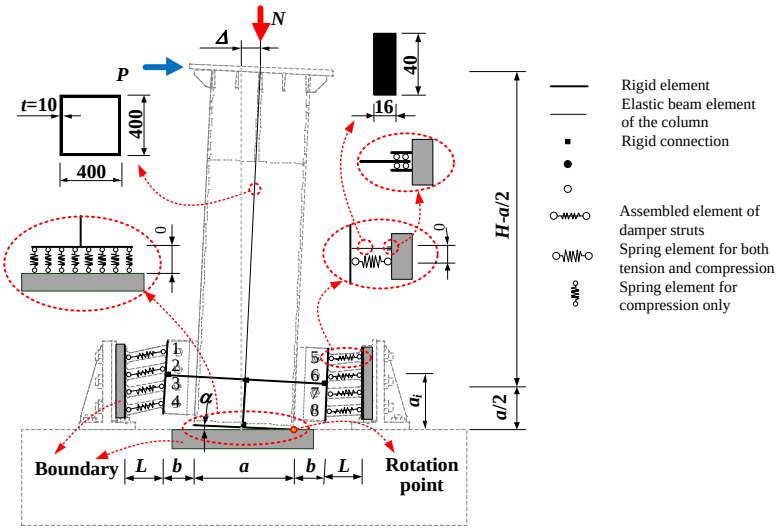

Fig. 4 – Simplified model of the IRR column

Based on these assumptions, we can obtain the axial deformation of the struts and relative rotation angle between the strut boundaries, using simple geometry, as shown in Fig. 5.

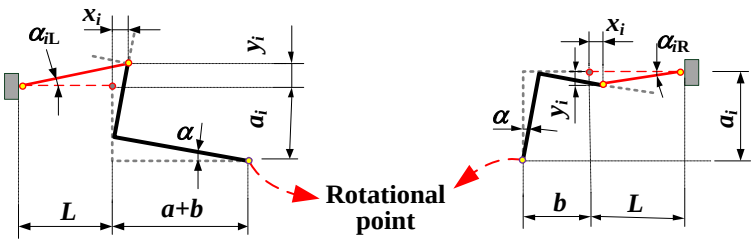

(a) Damper L (b) Damper R

Fig. 5 – Deformation for struts

For dampers at the left side of the column (Damper L), the axial deformation of the struts can be obtained from Eq. (1~3):

$$x_i = a_i \sin\alpha + (a+b)(1-\cos\alpha) \tag{1}$$

$$y_i = a_i(\cos\alpha - 1) + (a+b)\sin\alpha \tag{2}$$

$$\delta_i = \sqrt{(x_i + L)^2 + y_i^2} - L \tag{3}$$

where x_i and y_i are the horizontal and vertical displacement of the ith strut nodes near the column side, respectively; δ_i is the axial deformation of the ith strut (i=1-8, as labeled in Fig. 4); a_i is height of the ith strut from its centroid to the top of the foundation.

For dampers at the right side of the column (Damper R), the axial deformation of the struts can be obtained from Eq. (4~6):

$$x_i = a_i \sin\alpha + b(\cos\alpha - 1) \tag{4}$$

$$y_i = a_i(1 - \cos\alpha) + b\sin\alpha \tag{5}$$

$$\delta_i = L - \sqrt{(L - x_i)^2 + y_i^2} \tag{6}$$

The elastic potential energy of each damper strut due to axial deformation and boundary rotation can be calculated from Eq. (7~8), respectively:

$$E_{k\delta i} = \frac{EA}{2L}\delta_i^2 \tag{7}$$

$$E_{k\alpha i} = \frac{2EI}{L}\alpha_i^2 \tag{8}$$

Based on the principle of energy conservation and ignoring the axial deformation of the steel column due to flexural deformation, the external work done by horizontal and axial load equals to the internal work, which gives:

$$\sum E_{k\alpha i} + \sum E_{k\delta i} + E_c = \frac{1}{2}P(\Delta_R + \Delta_c) - N\frac{a}{2}\alpha \tag{9}$$

The negative sign of N indicates that the direction of axial load is opposite to the direction of its displacement. Since we also have

$$E_c = \frac{1}{2}P\Delta_c \tag{10}$$

Substituting Equation (1~8) and (10) into Equation (9), the horizontal load carrying capacity of the IRR column can be obtained as follows:

$$P = \frac{2(\Sigma E_{k\alpha i} + \Sigma E_{k\delta i})}{\Delta_R} + \frac{Na}{H} \tag{11}$$

The horizontal displacement due to the flexural deformation of the steel column caused by this horizontal load will be:

$$\Delta_c = \frac{PH^3}{3EI_c} \tag{12}$$

The stiffness of the IRR column will then be:

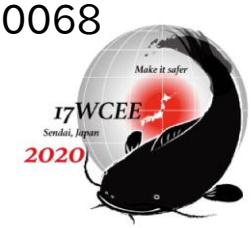

$$K_e = \frac{P}{\Delta_R + \Delta_c} \tag{13}$$

4. Verification of the equations

Using the proposed equations, the initial stiffness of a specified IRR column can be calculated with a given deformation, either the uplift angle of the steel column α or the horizontal displacement Δ. To avoid equation iteration, it is suggested to start with a small value of α, such as 1/1000. The initial stiffness of the IRR columns tested by Liu et al (Liu et al. (2019)[18]) were calculated with the actual parameters and listed in Table 1, where t is the thickness of the damper; λ, n and N_k are the shear-to-depth ratio, axial compression ratio and applied axial load of the columns, respectively; K_{TEST} and K_{FEM} are the initial stiffness of the columns obtained from the first cycle of the hysteretic curves from test and finite element analysis, respectively; K_c is the elastic stiffness of the steel column without dampers and with a fixed end at the foundation.

It can be seen from Table 1 that the calculated value of K_e is much higher than the tested value K_{TEST}, because there were different kinds of slippages during the test, including slippages between the connecting plates and the dampers, T-studs and foundation, foundation and the pedestals, et al, while the proposed method did not take these slippages into consideration. The more severe the slippages are, the bigger the differences between tested and calculated values become. Three-dimensional FE models were established, considering the interaction between the connecting plates, dampers and high strength bolts, and verified with test results. The overall performance of the IRR columns obtained from FE analysis agreed well with the test, suggested in Fig. 3(b) for specimen S16-5.5-0.1. More detailed information of the FE analysis of the IRR columns can be found in Liu et al (Liu et al. (2019) [22]). The initial stiffness of the IRR columns obtained from FE analysis is higher than that from test mainly because of the simplification of the material and idealization of the specimen dimensions. Hence the slippages in FE model were not as severe as that in the test and the values of K_{FEM} of the IRR columns are relatively close to those of K_e. The values of K_c are really close to those of K_e, suggesting that the initial stiffness of the IRR column is not weakened due to the fact that the column end is not fixed at the foundation.

Table 1 – Comparison of stiffness results with different method

Specimen I.D.	t (mm)	λ	n	N_k (kN)	K_{TEST} (kN/mm)	K_{FEM} (kN/mm)	K_c (kN/mm)	K_e (kN/mm)
S20-5.5-0.1-B	20	5.5	0.1	446	17.31	20.10	22.97	24.03
S20-5.5-0.1-A	20	5.5	0.1	446	12.64			
S16-5.5-0.1-B	16	5.5	0.1	446	11.45	19.37	22.97	23.26
S16-5.5-0.1-A	16	5.5	0.1	446	11.97			
S16-3-0.1	16	3.0	0.1	446	39.77	79.98	141.52	139.94
S16-3-0.2	16	3.0	0.2	893	34.10	101.90	141.52	158.60

For further understanding of the influence of different parameters to the initial stiffness of the IRR columns, parameter study using FE method was carried out and the results were summarized in Table 2.

Table 2 –Analysis matrix of FE modeling and calculated results

Specimen I.D.	t (mm)	$n=N/(f_yA)$	N_k(kN)	K_{FEM} (kN/mm)	K_c (kN/mm)	K_e (kN/mm)	K_e/K_{FEM}
S8-5.5-0.1	8	0.1	446	17.07	22.97	21.00	1.23

S8-5.5-0.2		0.2	892	22.29	22.97	23.62	1.06
S8-5.5-0.3		0.3	1339	25.99	22.97	25.12	0.97
S8-5.5-0.4		0.4	1784	28.12	22.97	26.08	0.93
S8-5.5-0.5		0.5	2230	28.79	22.97	26.76	0.93
S8-5.5-0.6		0.6	2676	29.16	22.97	27.26	0.93
S12-5.5-0.1	12	0.1	446	18.43	22.97	22.28	1.21
S12-5.5-0.2		0.2	892	23.20	22.97	24.32	1.05
S12-5.5-0.3		0.3	1339	26.68	22.97	25.56	0.96
S12-5.5-0.4		0.4	1784	28.58	22.97	26.39	0.92
S12-5.5-0.5		0.5	2230	29.13	22.97	26.98	0.93
S12-5.5-0.6		0.6	2676	29.49	22.97	27.42	0.93
S16-5.5-0.1	16	0.1	446	19.37	22.97	23.36	1.21
S16-5.5-0.2		0.2	892	23.85	22.97	24.90	1.04
S16-5.5-0.3		0.3	1339	27.20	22.97	25.94	0.95
S16-5.5-0.4		0.4	1784	28.94	22.97	26.65	0.92
S16-5.5-0.5		0.5	2230	29.40	22.97	27.18	0.92
S16-5.5-0.6		0.6	2676	29.76	22.97	27.58	0.93
S20-5.5-0.1	20	0.1	446	20.10	22.97	24.03	1.20
S20-5.5-0.2		0.2	892	24.37	22.97	25.37	1.04
S20-5.5-0.3		0.3	1339	27.58	22.97	26.26	0.95
S20-5.5-0.4		0.4	1784	29.23	22.97	26.88	0.92
S20-5.5-0.5		0.5	2230	29.63	22.97	27.35	0.92
S20-5.5-0.6		0.6	2676	29.90	22.97	27.71	0.93
						Average value	1.00
						Standard deviation	0.11

It can be seen from Table 2 that the calculation results using the proposed method agreed well with the FE analysis. The relationship of the calculated initial stiffness with damper thickness and axial compression ratio was shown in Fig. 6.

It can be seen that the calculated stiffness increases almost linearly with the increase of damper thickness and logarithmically with the increase of axial compression ratio.

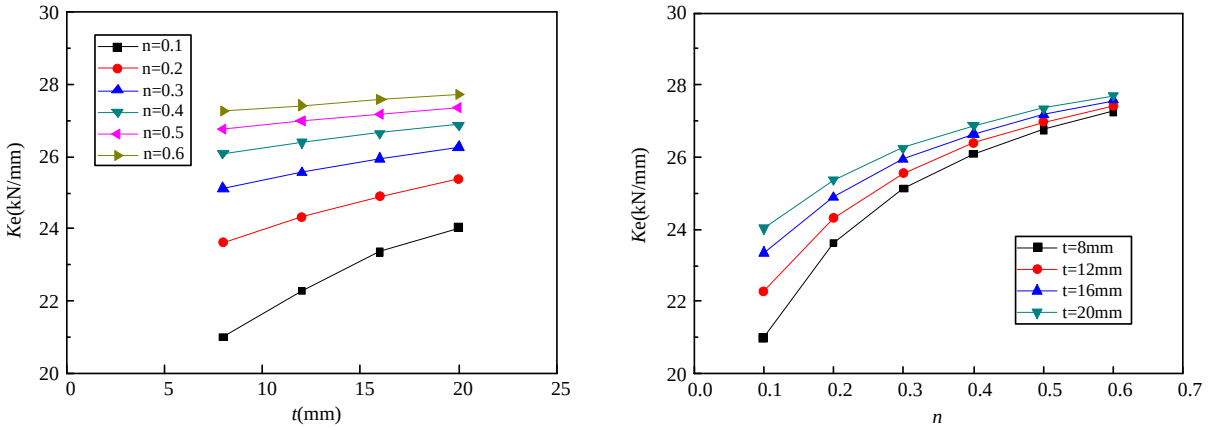

(a) K_e vs. t (b) K_e vs. n

Fig. 6 – Influence of t and n to K_e

5. Conclusion

An innovative resilient rocking (IRR) column was proposed and the deformation characteristics of such column under combined axial and horizontal load was introduced. This system, which was designed based on the "strong-column/weak- damper" philosophy, provides a valid optional technique to achieve resilience for moment-resisting frame structures, since all of the plastic deformation is concentrated within the replaceable steel slit dampers. A simplified model to calculate the initial stiffness of the IRR columns was proposed and verified using both test and FE results. The proposed equation provides a satisfactory prediction of the initial secant stiffness of the IRR columns.

6. Acknowledgements

This work was supported by the National Natural Science Foundation of China (Grant No. 51878304 and 51578254) and Natural Science Foundation of Fujian Province (Grant No. 2018J01074), which is gratefully acknowledged. The opinions in this paper are those of the writers and do not necessarily represent the views of the sponsors.

7. Copyrights

8. References

[1] El-Seikh M, Sause R, Pessiki S, Lu L. Seismic behavior and design of unbonded post-tensioned precast concrete frames. *PCI J* 1999; 44(3):54-71.

[2] Priestley M, Sritharan S, Conley J, Pampanin S. Preliminary results and conclusions from the PRESSS five-story precast concrete test buildings. *PCI J* 1999; 44(6):42-67.

[3] Ricles J, Sause R, Garlock M, Zhao C. Posttensioned seismic-resistant connections for steel frames. *J Struct Eng* 2001; 127(2):113-121.

[4] Ricles J, Sause R, Peng S, Lu L. Experimental evaluation of earthquake resistant posttensioned steel connections. *J Struct Eng* 2002; 128(7):850-859.

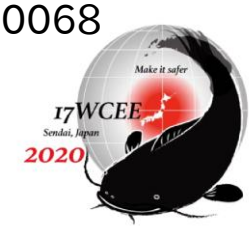

[5] Christopoulos C, Filiatrault A, Folz B, Uang CM. Posttensioned energy dissipating connections for moment-resisting steel frames. *J Struct Eng* 2002; 128(9):1111-1120.

[6] Dowden D, Bruneau M. Kinematics of Self-Centering Steel Plate Shear Walls with NewZ-BREAKSS Post-Tensioned Rocking Connection. *Engineering Journal*, Third Quarter 2016: 117 – 135.

[7] Fortney P, Shahrooz B, Rassati G. Large-scale testing of a replaceable "fuse" steel coupling beam. *J Struct Eng* 2007; 133(12):1801-1807.

[8] Shahrooz B, Fortney P, Harries K. Steel coupling beams with a replaceable fuse. *J Struct Eng* 2018; 144(2):04017210.

[9] Farsi A, Keshavarzi F, Pouladi P, Mirghaderi R. Experimental study of a replaceable steel coupling beam with an end-plate connection. *J Constr Steel Res* 2016; 122:138-150.

[10] Ji XD, Wang YD, Ma QF, Okazaki T. Cyclic Behavior of Replaceable Steel Coupling Beams. *J Struct Eng ASCE* 2017; 143:04016169.

[11] Ji XD, Liu D, Sun Y, Hutt CM. Seismic performance assessment of a hybrid coupled wall system with replaceable steel coupling beams versus traditional RC coupling beams. *Earthq Eng Struct D* 2017; 46:517-35.

[12] Shen Y, Christopoulos C, Mansour N, Tremblay R. Seismic design and performance of steel moment-resisting frames with nonlinear replaceable links. *J Struct Eng* 2011; 137(10):1107-1117.

[13] Oh S, Kim Y, Ryu H. Seismic performance of steel structures with slit dampers. *Engineering Structures* 2009; 31:1997-2008.

[14] Köken A, Köroğlu M. An experimental study on beam to column connections of steel frame structures with steel slit dampers. *Journal of Performance of Constructed Facilities* 2015; 29(2):04014066.

[15] Mansour N, Christopoulos M, Tremblay R. Experimental Validation of Replaceable Shear Links for Eccentrically Braced Steel Frames. *Journal of Structural Engineering* 2011; 137 (10) 1141-1152.

[16] Azhata T, Midorikawa M, Ishihara T, and Wada A. Simplified prediction method for seismic response of rocking structural systems with yielding base plates. *13th world conference on earthquake engineering* 2004; No.: 371. Vancouver, Canada.

[17] Eatherton M, Hajjar J. Hybrid simulation testing of a self-centering rocking steel braced frame system. *J Earthquake Eng Struct Dyn* 2014; 43(11):1725-1742.

[18] Liu Y, Guo Z, Liu X, Chicchi R, and Shahrooz B. An innovative resilient rocking column with replaceable steel slit dampers: experimental program on seismic performance. *Engineering Structures* 2019; 183:830-840.

[19] Climent A, Oh S, Akiyama H. Ultimate energy absorption capacity of slit-type steel plates subjected to shear deformation. *Bull math Statist* 1998; 28:115-126.

[20] Chan RWK, Albermani F. Experimental study of steel slit damper for passive energy dissipation. *Engineering Structures* 2008; 30:1058-1066.

[21] Lee J, Kim J. Development of box-shaped steel slit dampers for seismic retrofit of building structures. *Engineering Structures* 2017; 150:934-946.

[22] Liu Y, Liao Y, Guo Z, Lu Y, Liu X, Shahrooz B. Seismic performance of an innovative composite column with replaceable steel slit dampers: FEM analysis and design method. *8th International Conf on Composite Construction in Steel and Concrete* 2017; Jackson Hole, US.

